Sudipta Patra · Subhasis Sinha ·
G. S. Mahobia · Deepak Kamble *Editors*

Proceedings of the International Conference on Metallurgical Engineering and Centenary Celebration

METCENT-2023, 26–28 October, Varanasi, India

MOREMEDIA

Springer

Proceedings of the International Conference on Metallurgical Engineering and Centenary Celebration

Sudipta Patra · Subhasis Sinha · G. S. Mahobia · Deepak Kamble
Editors

Proceedings of the International Conference on Metallurgical Engineering and Centenary Celebration

METCENT-2023, 26–28 October, Varanasi, India

Springer

Editors
Sudipta Patra
Department of Metallurgical Engineering
IIT(BHU)
Varanasi, India

Subhasis Sinha
Department of Metallurgical Engineering
IIT(BHU)
Varanasi, India

G. S. Mahobia
Department of Metallurgical Engineering
IIT(BHU)
Varanasi, India

Deepak Kamble
Department of Metallurgical Engineering
IIT(BHU)
Varanasi, India

ISBN 978-981-99-6862-6 ISBN 978-981-99-6863-3 (eBook)
https://doi.org/10.1007/978-981-99-6863-3

This Springer imprint is published by the registered company Springer Nature Singapore Pte Ltd.
The registered company address is: 152 Beach Road, #21-01/04 Gateway East, Singapore 189721, Singapore

Paper in this product is recyclable.

Preface

The Department of Metallurgical Engineering, Indian Institute of Technology (BHU), Varanasi, India, was established in the year 1923 and has completed 100 glorious years in 2023. The first ever undergraduate program in Metallurgy in India was started here in 1923, and the department was also among the oldest in the country to award PhD and M.Tech degrees in 1955 and 1957, respectively. Till date, 2794 B.Tech, 692 postgraduates (including M.Tech and dual degree) and 197 Ph.D. scholars have graduated from the department.

An international conference named METCENT 2023 was held from 26–28th October 2023 to celebrate this auspicious occasion. The conference was attended by around 300 delegates consisting of academicians and industry professionals including several alumni of the department. More than 150 oral and poster presentations were made at the conference spread over five technical sessions.

The conference program comprised of five technical sessions covering the areas of Extractive metallurgy, Mechanical Behaviour, Physical Metallurgy and Characterization, Modelling and Simulations, Functional Materials, Welding, etc. Five Plenary speakers delivered lectures at the conference. The Plenary talks discussed the "use of biogas in iron and steel making", "Nano-Engineered Materials", "Computationally designed alloys", "novel nitrides and Chalcogenide materials" and "Iron making without using fossil fuel".

This proceeding contains 33 original research papers and five review papers covering various areas of metallurgical and materials research. The full research papers are categorized into Ferrous Process Metallurgy (eight papers), Computational Materials Science (seven papers), Advanced Materials (five papers), Development and Characterization of Steels (five papers), Processing and Structure-Property Correlation (six papers) and Review (five papers). Fifty-five manuscripts were received, out of which 38 were accepted for publication in the current proceeding.

We would like to thank all the members of the conference organizing committee, sponsors, authors, presenters, session chairs, student volunteers, delegates and reviewers for their support and contribution in making this event successful

October 2023

Sudipta Patra
Subhasis Sinha
G. S. Mahobia
Deepak Kamble

Organization

Members

Rajiv Kumar Mandal
Nilay Krishna Mukhopdhyay
N. C. Santhi Srinivas
B. Nageswara Sarma
Kamalesh Kumar Singh
Chhail Kumar Behera
Rampada Manna
Kausik Chattopadhyay
Joysurya Basu
Vikas Jindal
Jayant Kumar Singh
Nand Kishore Prasad
Ashok Kumar Mondal
Bratindranath Mukherjee
Randhir Singh
Surya Deo Yadav
Subhasis Sinha
Sree Harsha Nandam
Deepak Kamble
Lakhindra Marandi
Praveen Sathiyamoorthi
Ameya K. Kadrolkar
L. Sankara Rao
Arun P. Singh
Rana P. Yadav
Pramod Kumar Jain (Patron)
Sunil Mohan (Chairman)
Girija Shankar Mahobia (Convener)
Sudipta Patra (Treasurer)

Advisory Committee

Alberto Conejo	Morelia Technological Institute, Mexico
S. Seetharaman	Royal Institute of Technology, Sweden
Paulo Santos Assis	Universidade Federal de Ouro Preto, Brazil
Amit Chakravarty	National Water Company, Saudi Arabia

Antonello Astarita	University of Naples “Federico II”, Italy
Amit Misra	University of Michigan, USA
K. Linga (KL)	Murty NC State University, USA
Fathi Habashi	Laval University, Canada
Kedar Nath Gupta	.
J. Paulo Davim	The University of Aveiro (UA), Portugal
Rajeshwar P. Wahi	Technical University Berlin
E. N. Suleimenov	Kazakh-British Technical University, Republic of Kazakhstan
Pallav Chattopadhyay	Lincoln Electric, Deutschland GmbH, Germany
Lokesh Kumar Singhal	California, USA
Govind S. Gupta	IISc Bangalore
Tata Narasinga Rao	ARCI, Hyderabad
K. Narasimhan	IIT Bombay
S. K. Jha	MIDHANI, Hyderabad
Sanjay Sharma	L&T Special Steels & Heavy Forgings Pvt. Limited, Surat
A. Nagesha	IGCAR, Kalpakkam
T. A. Abinandanan	IISc Bangalore
B. P. Kashyap	IIT Jodhpur
R. C. Gupta	IIT (BHU) Varanasi
T. R. Mankhand	IIT (BHU) Varanasi
S. Lele	IIT (BHU) Varanasi
Vakil Singh	IIT (BHU) Varanasi
Paresh Haribhakti	TCR Advanced Pvt Ltd., Vadodara
Manish Raj	Jindal Steel and Power, Raigarh
Narayana Murty	SVS, Liquid Propulsion Systems Centre, Trivandrum
Amit Rastogi	Institute of Medical Sciences (BHU), Varanasi
Dhiren Kumar Panda	JSW Steel & Coated Products Vidyanagar

Contents

Ferrous Process Metallurgy

Development of a Low Silica Calcium Aluminate Based Mould Flux for Casting High Al/Mn Steels

Aman Nigam(✉) and Rahul Sarkar(✉)

Indian Institute of Technology, Kanpur, India
{amann21,rsarkar}@iitk.ac.in

Abstract. The third generation of AHHS is a new type of advanced high-strength steel that has improved ductility and can be used in a variety of applications in automobiles. Because of its high Al (0.5–2 wt.%) % and Mn (5–7 wt.%) contents, Al and Mn easily react with the oxides such as SiO_2 present in the conventional calcium silicate mold flux which affects the lubrication and crystallization ability provided by the slag film resulting in casting defects such as Break Out Prediction (BOP) alarms, Transverse and Longitudinal depressions. In this study, a calcium aluminate-based alternative mold flux containing different fluxing agents (Na_2O, B_2O_3, SiO_2, and CaF_2) has been developed. Using a differential scanning calorimeter (DSC/DTA) at three different heating rates, 10 K/min, 15 K/min, and 20 K/min, the onset and peak temperatures of crystallization for the composition having $w(CaO)/w(Al_2O_3) = 1$ were determined. The melt structure of the vitreous calcium aluminate-based mold flux was also examined using Raman spectroscopy, and it was shown to have several $[AlO_4]$ structural units with $[BO_3]$ pyroborate units. The deconvolution results of Raman spectra reveal the degree of polymerization (DOP) of the aluminosilicate network present in calcium aluminate-based mold flux. Utilizing structural data such as the area fraction of various structural units found in the melt structure allowed us to examine the tendency of these fluxes to crystallize.

Keywords: AHSS · Mould Flux · Melt Structure · Degree of Polymerization · Raman Spectroscopy

1 Introduction

The continuous casting of steel requires the use of mold flux or casting powders. These mould fluxes usually contain CaO and SiO_2 as their major components with further addition of fluxing agents to engineer the properties required for the steel to be cast. During the continuous casting of steel, the mold flux spreads out on the steel meniscus at the top of the mold, forming a powder bed. These powders warm up and finally melt, creating a pool of slag as shown in Fig. 1. This slag pool acts as a reservoir that infiltrates between the solidified steel shell and the water-cooled copper mold as the mold descends. The slag partially solidifies to create a slag film that is made up of a liquid layer (0.1–0.3 mm thick) and a solid layer (1–2 mm thick) (Fig. 1). Due to the

S. Patra et al. (Eds.): METCENT 2023, *Proceedings of the International Conference on Metallurgical Engineering and Centenary Celebration*, pp. 3–12, 2024.
https://doi.org/10.1007/978-981-99-6863-3_1

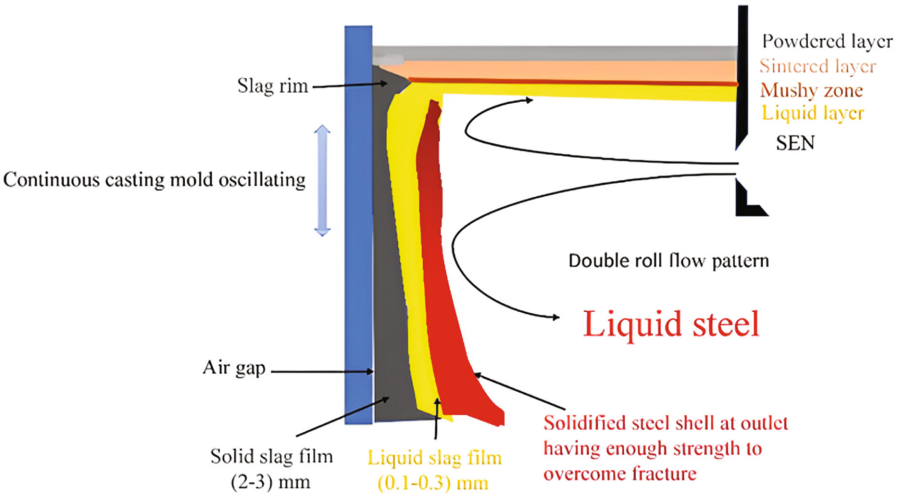

Fig. 1. Schematic diagram illustrating the function of mold flux in continuous casting.

rapid cooling, the slag layer will initially be glassy, but as time passes, the proportion of crystalline phases steadily rises until it achieves a stable state. The amount of lubrication provided to the shell is determined by the thickness of the liquid slag film. The amount of heat extracted from the shell is controlled by how thick the solid layer is and how much of it is crystalline. In addition to lubrication and heat extraction, the mold flux protects the steel from oxidation and prevents freezing by acting as thermal insulation on the top of the steel meniscus.

The third generation of AHHS is a new type of advanced high-strength steel that has improved ductility and can be used in a variety of applications in automobiles. Because of its high Al (0.5–2 wt.%) % and Mn (5–7 wt.%)[1], Al and Mn easily react with the oxides such as SiO_2 present in the conventional CaO-SiO_2-based mold flux [Eq. (1)-(2)] resulting in an increase in the viscosity and melting temperature of the mold flux due to a sudden rise in the basicity and Al_2O_3/SiO_2 ratio[2], which in turn will deteriorate the crystallization and lubrication provided by the slag film causing a variety of issues and flaws, including BOP (Break Out Prediction) alarms, transverse and longitudinal depressions.

$$3(SiO_2) + 4[AI] = 3[Si] + 4(AI_2O_3) \tag{1}$$

$$3(MnO)+2[AI]= 3[Mn]+2(AI_2O_3) \tag{2}$$

Numerous research has concentrated on the crystallization and lubricating tendencies of mold fluxes since they offer a proper understanding of the flux, which will help remove casting flaws. As a consequence, there is an increasing demand for utilizing calcium aluminate-based mold powders for casting high Al/Mn steels replacing conventional calcium silicate-based mold powders. The calcium aluminate mold fluxes contain little or no Silica present in them called “Non-Reactive” mold flux. The only problem with

using this kind of mold flux is that it melts at a high temperature, which contradicts the purpose of using it. Several fluxing agents, such as Li_2O, Na_2O, B_2O_3, and MgO, are added to these mold fluxes to adjust their melting points to a desirable range and may also increase their ability to crystallize and lubricate. In the same context Gao et al.[3] developed a calcium aluminate mold flux with a low amount of silica having a certain addition of Na_2O which will eventually help in the enhancement of crystallization tendency and also will lead to the depolymerization of the melt structure. In their study of the non-isothermal crystallization kinetics of the non-reactive F-free mold flux, Shu et al.[4] found that the tendency for crystallization increased with an increase in the ratio of w(CaO)/w(Al_2O_3) for constant B_2O_3 and Na_2O. Ryu et al.[5] investigated the impact of basicity and the alumina content on crystallization temperature and incubation period. They discovered that as the Al_2O_3 and C/S ratio increased, the temperature of crystallization increased while the incubation period decreased. According to Zhou et al.[6], the capacity to crystallize the mold powder utilized in the casting of high-Al steels was found to be initially increased and then inhibited with increasing Al_2O_3 concentration.

The tendency of the mold flux to crystallize is widely dependent on the melt structure of the mold fluxes which can be observed through various spectroscopic techniques like FTIR, Raman & NMR spectroscopy. Several researchers tried to explain the effect of crystallization with the help of the degree of polymerization (DOP) of the melt structure[6]. The amount of bridging and non-bridging oxygen in the melt structure corresponds to the degree of polymerization. The tendency of the mold flux for crystallization increases as the DOP of the structure decreases, and vice versa. Shu et al. [7] looked at how the structure of the melt affected the crystallization of F-free mold flux. The results showed that as the amount of Na_2O in the mold flux increases, the DOP of the melt structure decreases, making it easier to crystallize.

To prevent interfacial reactions and to achieve a proper balance between mold flux lubrication and heat extraction ability, the objective of this research is to create a specific type of mold flux that is suitable for third-generation AHSS steel with a high Al/Mn content. A non-reactive CaO-Al_2O_3-based mold flux with little to "No Silica" or by altering the w(CaO)/w(Al_2O_3) & basicity ratio in conventional mold flux can be used to achieve this goal.[8].

2 Experimental Methodology

2.1 Preparation of Mold Fluxes

Reagent-grade chemicals of CaO, Al_2O_3, Na_2CO_3, SiO_2, CaF_2, and B_2O_3 with a purity of 99.99% were used as raw materials to prepare mold flux samples used in this investigation. They have compositions according to Table 1. Na_2CO_3 was calcinated to Na_2O at 873 K for 2 h in the air to remove moisture. The raw materials were thoroughly mixed in an agate mortar before being heated and melted in a graphite crucible inside the muffle furnace at 1673 K for one hour. The pre-melted samples were then pulverized into powder for observation in X-Ray Diffraction (XRD: PANanalytical Empyrean), Induced Coupled Plasma-Mass Spectroscopy (ICP-MS), and X-Ray fluorescence (XRF) after being quenched in a bucket of water to produce an altogether amorphous phase. XRD

aims to study the phases in the phases formed in the mold fluxes and thus to determine the crystallinity whereas ICP-MS & XRF were used to determine the chemical composition of pre-melted samples so that there should not be any significant evaporation loss.

Table 1. Chemical constitution of the mold flux

Composition in weight %						
Sample	CaO	Al_2O_3	Na_2O	B_2O_3	SiO_2	CaF_2
w(CaO)/w(Al_2O_3)=1	35	35	15	5	5	5

2.2 Measurements Using DSC

Glassy samples were ground up and analyzed through a DSC analysis. With argon serving as the purge gas under dynamic conditions, the measurements were carried out using a thermal analyzer, model STA 2500 Regulus from the manufacturer Netzsch. To reduce sample volatile loss, platinum crucibles with platinum covers were used. The baseline was created using empty platinum crucibles exposed to variable heating rates (20 K/min, 15 K/min, and 10 K/min).

2.3 Raman Spectroscopy

The melt structure of the slag was determined by Raman spectra analyses on the ground-up quenched samples at room temperature. The Raman spectrometer (Princeton Instruments Acton Spectra Pro 2500i) was utilized to capture the Raman spectra in the frequency range of (100–2500 cm^{-1}) using a 532 nm (DPSS Laser (Laser Quantum gem 50 mw)) wavelength laser as the excitation source. However, the Raman shifts were mainly concentrated between (300–1700) cm^{-1} which is important for defining the structure of the slag samples. The baseline subtraction was done in the origin and the spectra were deconvoluted by the Gaussian functions with a minimum correlation coefficient of $R^2 \geq 0.969$. The area fraction of the observed peaks was used to compute the abundance or population of the structural units.

3 Results and Discussion

3.1 Sequence of Crystal Precipitation

Figure 2 displays the DSC data for the mold flux system having a w(CaO)/w(Al_2O_3) ratio of 1, for various heating rates between 20 K/min and 10 K/min. The thermographs shown represent the exothermic crystallization peak (Exothermic occurs in a downward direction). Table 2 shows the onset and peak temperatures for the first and second crystallization events (Peak 1 and Peak 2) for the w(CaO)/w(Al2O3) = 1 slag sample. The

peak analysis in the Origin 2021b software was used to determine the various temperatures listed in Table 2. The temperature at which crystallization first starts during a non-isothermal crystallization process correlates to the crystallization temperature for the crystalline phase, which can be identified as the temperature at which exothermic peaks first appear during heating. The onset and the peak temperature of a particular crystallization event depend upon the heating rate provided, as the transition from glass to a crystal phase is dependent on the nucleation and growth rate. The glass phase provides ample time for nucleation and crystal growth when the heating rate is low, resulting in a comparatively low crystallization temperature. Higher heating rates result in shorter times for crystal nucleation and growth. The crystallization temperature will be higher when the rate of transition from the glass phase to the crystal phase is at its highest[9]. When the sample is heated to the various target temperatures listed in Table 2, XRD and SEM/EDS will figure out the order in which different crystals form.

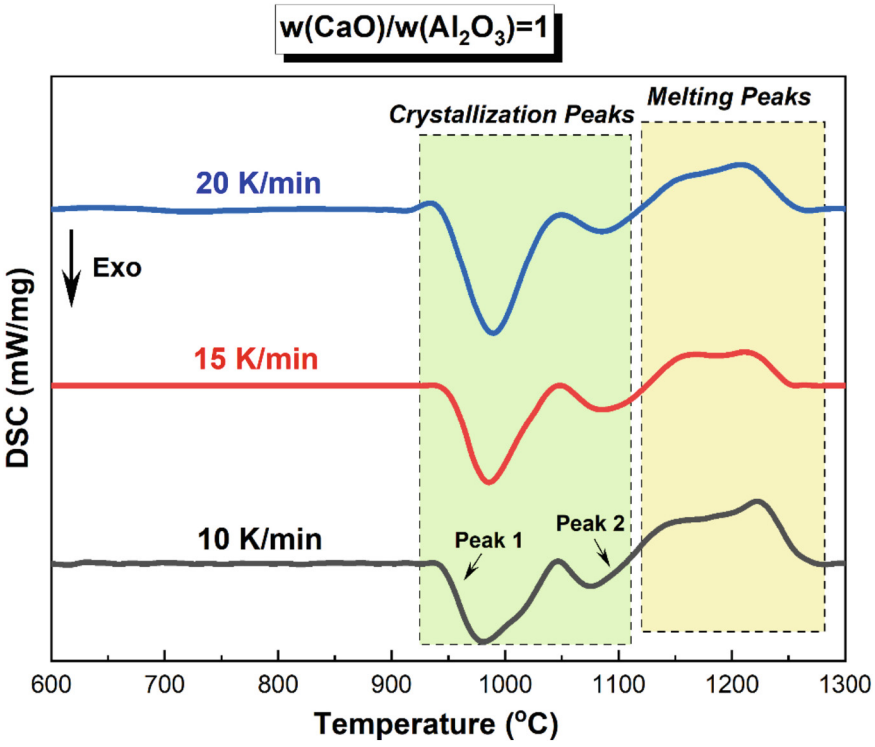

Fig. 2. DSC curve of w(CaO)/w(Al_2O_3) = 1 sample at different heating rates

Table 2. Onset and Peak temperature at different heating rates

Crystallization Events		Heating Rates		
Peak Information (°C)		10 K/min	15 K/min	20 K/min
Peak 1	Onset Temperature	934	936	938
	Peak Temperature	981	986	990
Peak 2	Onset Temperature	1045	1049	1046
	Peak Temperature	1076	1086	1089

3.2 Raman Spectroscopy

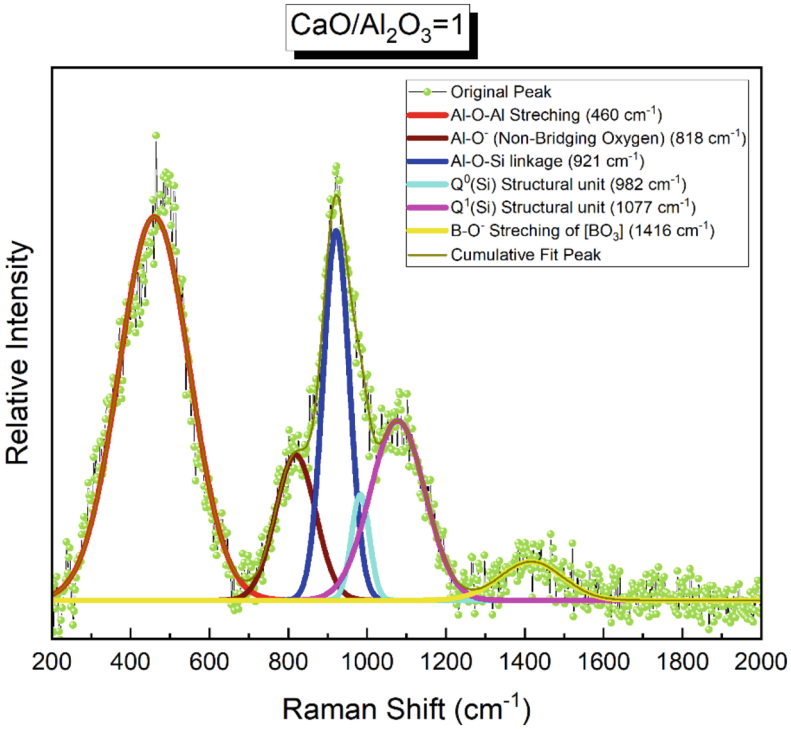

Fig. 3. The deconvoluted Raman spectra of $w(CaO)/w(Al_2O_3) = 1$

The melt structure of the calcium aluminate-based mold fluxes can be related to its viscosity and the crystallization tendency which in turn can influence how well the mold fluxes lubricate and transfer heat to the steel shell. The structural functionality

performed by the Al_2O_3 in the melt structure is complicated as it is amphoteric. In other words, the number of constituents in the slag system correlates to its structural role. These components can be network formers or network breakers depending on the type of steel to be cast. To comprehend the melt structure of the calcium aluminate slag system and how the structure changes as SiO_2 is replaced by Al_2O_3, many studies have been conducted.

As mentioned above transition from the calcium silicate slag system to the calcium aluminate slag system will typically lead to a more intricate melt structure. It is indicated that Al_2O_3 mainly exists in the form of $[AlO_4]^{5-}$,.$[AlO_5]^{7-}$, and.$[AlO_6]^{9-}$ structural units in the melt structure. These units can act as network former or network breakers depending on the composition of Al_2O_3 present in the slag system. It is to be said that when the Al_2O_3 is present in the low composition in the calcium silicate mold flux it may behave as a network breaker in the form of $[AlO_5]^{7-}$ and.$[AlO_6]^{9-}$ structural units but as the composition of Al_2O_3 increases to a certain extent these structural units will be converted to $[AlO_4]^{5-}$ units and the Al_2O_3 will act as the network former. During this whole transition as the silicate structure changes to an aluminate structure, the structural units present in the silicate structure in the form of the $[SiO4]^{4-}$ will be transformed to the linkages like Al-O^0 (O^0 denotes the bridging oxygen) and Al-O-Si, with the aid of certain basic oxides like CaO, Na_2O, Li_2O, MgO & BaO. This will result in the depolymerization of the silicate structure which will eventually be transformed into the aluminate structure[9]. Thus the complexity of the melt structure will be enhanced and this will introduce variable crystalline phases.

Several researchers reported that in the calcium aluminate slag system with the increase in w(CaO)/w(Al_2O_3) ratio, the bridging.oxygen present in the form of Al-O^0 and Al-O-Si linkages will be destroyed and will be transformed to Al-O^-(.O^- is the bridging oxygen) also the silicate units present having higher polymerization degree in the form of Q^1(Si) and Q^2(Si) will be destroyed to the lower polymerization degree i.e. to the Q^0(Si) structural unit (the number in the superscript denotes the quantity of bridging oxygen in the $[SiO_4]^{4-}$ unit). Furthermore, with the aid of O^{2-} (free oxygen) generated by added CaO or Na_2O, the network former unit $[AlO_4]^{5-}$ will be transformed into the network breaker units (Eqs. 3–5) $[AlO_5]^{7-}$, $[AlO_6]^{9-}$ [10].

$$[AlO_4]^{5-} + 2\,O^{2-} \leftrightarrow [AlO_6]^{9-} \tag{3}$$

Yang et al. reported that adding B_2O_3 to the calcium aluminate mold flux system has the exact opposite effect to that of adding Na_2O.[10] The Raman spectra of CaO-Al_2O_3–7 wt.% SiO_2 illustrate the $[BO_4]$ related 3D pentaborate structure, where $[BO_4]$ units are connected to the borate structures and.$[AlO_4]^{5-}$ tetrahedral unit. When B_2O_3 is added, there will be more of these units and links as $[BO_4]$ units promote the transition of higher polymerization structural units to lower polymerization structural units. It indicates that the B_2O_3 will behave as the network former in the calcium aluminate slag system. So, it will make the structure of the melt more intricate as well as raise the degree of polymerization. But, in the case of adding Na_2O, the O^{2-} that is given off will cause the aluminosilicate structure to change from bridging oxygen (O^0) to non-bridging oxygen (O^-) (Eq. 4), which will make the structure of the melt less complicated. Similar findings were made by Wang et al. for the CaO-Al_2O_3–10 wt% SiO_2-based slag system

with varying Na_2O composition, where it was found that the aluminosilicate structure depolymerization would be further enhanced with an increase in Na_2O content.

$$BO + O^{2-} \leftrightarrow 2NBO \tag{4}$$

To analyze the change in the degree of polymerization of the aluminate or aluminosilicate network Raman spectroscopy was collected for the present mold fluxes. The original Raman spectrums of all samples are shown in Fig. 3.

The spectra pattern around 460 cm^{-1} (lies in the low-frequency region of the Raman spectra) is corresponding to Al-O-Al stretching characteristics peak representing the bridging oxygen in the aluminate network having $[AlO_4]^{5-}$ unit. The mid-frequency region (700–1300 cm^{-1}) of the spectra shows the depolymerization of the aluminosilicate structure denoting $Al\text{-}O^-$ or $Si\text{-}O^-$ (O^- indicates the depolymerization of the network) telescopic vibrations as shown in the figure. The characteristics peak at 818 cm^{-1} and 921 cm^{-1} stand for the symmetric.$Al\text{-}O^-$ and Al-O-Si bonds, respectively. The degree of polymerization or depolymerization is represented by Q^n (n represents that number of bridging oxygen), where Q^0 refers to $[AlO_4]^{5-}$ or $[SiO_4]^{4-}$ unit. The structural units Q^0(Si), and Q^1(Si) correspond to the peaks at 982 cm^{-1} and 1077 cm^{-1} respectively.

$$[AlO_4]^{5-} + O^{2-} = [AlO_5]^{7-} \tag{5}$$

The band at 1416 cm^{-1} is attributed to the symmetric stretching vibrations of terminal oxygen atoms in orthoborate units $[BO_3]$, which means that B^{3+} is mainly forming $[BO_3]$ groups in the mold flux.

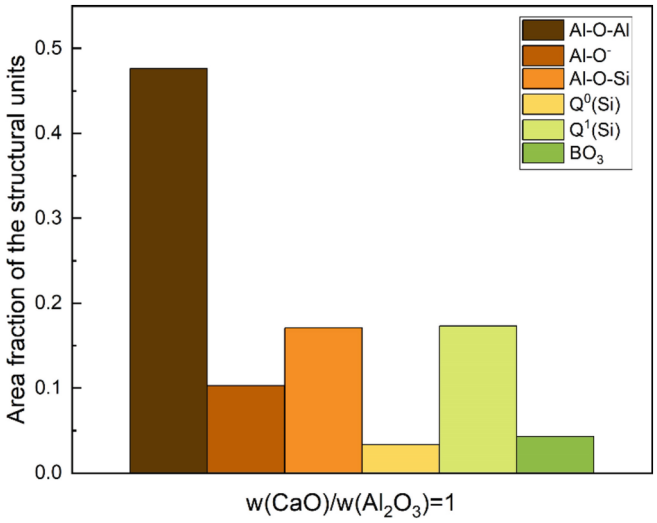

Fig. 4. Area fraction of the various structural units

The area fraction of the structural units determines the approximate population density of that unit, and this has been found out with the help of the area integration results

of the deconvoluted Raman spectra of the various units. Figure 4 shows that these results suggest that the depolymerization of aluminate and silicate structures happens when specific network breakers are added. This means that more complicated aluminate and silicate structures are turned into simpler ones when more CaO and Na_2O are added to the melt structure as they will release more O^{2-} ions. This is to say that by adding more Na_2O or increasing the C/A, the depolymerization of the aluminosilicate structure increases, which aids in crystallization because the crystallization temperature rises.

4 Conclusion

The crystallization tendency and the subsequent melt structure were studied for the low Silica calcium aluminate mold fluxes and the following conclusions can be drawn:

1) The onset crystallization temperature is rising with the heating rate, which means that at higher heating rates, the crystallization tendency will also rise. This will aid in the extraction of heat from the solidified steel shell, but it will also result in the formation of a slag rim, which will affect the infiltration of slag into the space between the solidified steel shell and slag film.
2) The depolymerization of the aluminate and silicate structure by the addition of Na_2O is revealed by Raman spectroscopy of the mold slag. A solid-state ^{27}Al NMR study will be used in the later part of this study to determine the type of structural units, whether they are $[AlO_4]$, $[AlO_5]$, or $[AlO_6]$ in the aluminate structure. NMR will also be used to look at the impact of fluorine on the structure.
3) To find out if adding Al_2O_3 to the mold flux will act as a network-forming agent or a network-breaking agent, the link between the structure of the melt and the ability of the mold flux to crystallize must be determined in the later stages of this study.

Acknowledgment. The author would like to express gratitude to the several labs at the Department of Materials Science and Engineering at IIT Kanpur for providing the various facilities needed for the current research.

References

1. Aydin, H., Essadiqi, E., Jung, I.H., Yue, S.: Development of 3rd generation AHSS with medium Mn content alloying compositions. Mater. Sci. Eng. A **564**, 501–508 (2013). https://doi.org/10.1016/j.msea.2012.11.113
2. Kim, M.S., Lee, S.W., Cho, J.W., Park, M.S., Lee, H.G., Kang, Y.B.: A reaction between high Mn-High Al Steel and CaO-SiO2-type molten mold flux: part I. composition evolution in molten mold flux. Metall. Mater. Trans. B **44**(2), 299–308 (2013). https://doi.org/10.1007/s11663-012-9770-z
3. Gao, J., Wen, G., Sun, Q., Tang, P., Liu, Q.: The influence of Na2O on the solidification and crystallization behavior of CaO-SiO2-Al2O3-based mold flux. Metall. Mater. Trans. B **46**(4), 1850–1859 (2015). https://doi.org/10.1007/s11663-015-0366-2
4. Shu, Q., Li, Q., Medeiros, S.L., Klug, J.L.: Development of non sreactive f-free mold fluxes for high aluminum steels: non-isothermal crystallization kinetics for devitrification. Metall. Mater. Trans. B **51**(3), 1169–1180 (2020). https://doi.org/10.1007/s11663-020-01838-4

5. Ryu, H.G., Zhang, Z.T., Cho, J.W., Wen, G.H., Sridhar, S.: Crystallization behaviors of slags through a heat flux simulator. ISIJ Int. **50**(8), 1142–1150 (2010). https://doi.org/10.2355/isijinternational.50.1142
6. Zhou, L., Wu, H., Wang, W., Luo, H., Li, H.: Crystallization behavior and melt structure of typical CaO–SiO2 and CaO–Al2O3-based mold fluxes. Ceram. Int. **47**(8), 10940–10949 (2021). https://doi.org/10.1016/j.ceramint.2020.12.213
7. Shu, Q., Klug, J.L., Medeiros, S.L.S., Heck, N.C., Liu, Y.: Crystallization control for fluorine-free mold fluxes: effect of Na2O content on non-isothermal melt crystallization kinetics. ISIJ Int. **60**(11), 2425–2435 (2020). https://doi.org/10.2355/isijinternational.ISIJINT-2020-132
8. Zhang, L., Wang, W.L., Shao, H.Q.: Review of non-reactive CaO–Al2O3-based mold fluxes for casting high aluminum steel. J. Iron Steel Res. Int. **26**(4), 336−344 (2019). https://doi.org/10.1007/s42243-018-00226-2
9. Wang, W., Xu, H., Zhai, B., Zhang, L.: A Review of the melt structure and crystallization behavior of non reactive mold flux for the casting of advanced high strength steels. Steel Res. Int. **93**(3), 1 (2022). https://doi.org/10.1002/srin.202100073
10. Yang, J., et al.: Effect of B2O3 on crystallization behavior, structure and heat transfer of CaO-SiO2-B2O3-Na2O-TiO2-Al2O3-MgO-Li2O mold fluxes. Metall. Mater. Trans. B **48**(4), 2077–2091 (2017). https://doi.org/10.1007/s11663-017-0997-6

Some Aspects of the Chemistry of Slags Containing Cr and V

Seshadri Seetharaman(✉)

Emeritus Royal Institute of Technology, Stockholm, Sweden
raman@kth.se

Abstract. The present paper provides some pioneering experimental information regarding the chemistry of steelmaking slags containing Cr and V. Initially, the thermodynamic activities of CrO and $VO_{1.5}$ in slags at very low oxygen potentials were determined by gas-equilibration technique involving CO-CO_2-Ar gas mixtures at 1600 °C. While the activity of CrO as a function of X_{CrO} showed a positive deviation from ideality, the trend in the case of $VO_{1.5}$ was found to be the opposite. In the case of Cr-slags, it is important to determine the valence states of Cr in the slag as a function of basicity, oxygen partial pressure prevailing and temperature. In view of the contradictory results in the literature, experiments were conducted by XANES (X-ray Absorption Near-Edge Spectroscopy) as well as the high temperature Knudsen cell mass spectroscopy (pioneering experiment). The ratio of Cr^{2+} /Cr^{3+} as functions of basicity, p_{O2} and temperature were determined. Cr emission from slags were determined by a thin film method, using SHTT (Single Hot Thermocouple Technique) set-up. It was found that at CrO_3 emissions are significant in air at steelmaking temperatures.

In the case of V-containing slags, the ratio of the valence states of vanadium was determined as functions of temperature and basicity by the same methods as in the case of Cr. The kinetics of evaporation of pure V_2O_5 was examined by thermogravimetry. Thin film experiments showed that vanadium losses as V_2O_5 are significant in oxidizing atmospheres. Further experiments were conducted by simultaneously applying vacuum and oxygen purging in order to force the micro bubbles of V_2O_5 formed and entrapped in the viscous slag. These experiments demonstrated the potential of this method to extract vanadium from slags, low grade ores and even pet-coke ash.

Keywords: Chromium · Slags · Steelmaking · Valences · Vanadium

1 Introduction

With the increasing need for light weight, high strength steel, the need for alloying elements has increased significantly world-wide. Correspondingly, the amounts of these valuable alloying elements are also lost as emissions in slags and dust. A study by the Swedish Steel Producers Association from 2012 showed (Table 1) that the amount alloying elements lost in emissions was higher than the amount needed for the production. This also has adverse impact on the environment apart from the economic losses.

S. Patra et al. (Eds.): METCENT 2023, *Proceedings of the International Conference on Metallurgical Engineering and Centenary Celebration*, pp. 13–18, 2024.
https://doi.org/10.1007/978-981-99-6863-3_2

Table 1. Amounts of alloying elements required annually and the amount lost to slag and dust 1.

Metal	Annual demand/t	Amount lost annually as waste emissions /t
Chromium	100 000	180 000
Manganese	50 000	70 000
Zinc	15 000	33 000
Nickel	25 000	17 500
Molybdenum	10 000	8 000

There is a strong need to optimize steelmaking processes and this requires an urgent need to understand the chemistry of the elements like Cr and V in steel slags. The present studies involved experimental studies of the thermodynamic activities of the oxides of Cr and V in as well as the valence states of these elements in the slags under steelmaking conditions by novel techniques. The emission of CrO_3 and V_2O_5 from thin films of slags at high temperature has been studied using a SHTT equipment. The present paper summarizes the efforts made at the Royal Institute of Technology, Stockholm in this direction. A part of the work was carried out in collaboration with the Institute for Iron and Steel Technology, Bergakademie, Freiberg, Germany.

Thermodynamic Activities of the Oxides of Cr^2 and V^3 in Slags

The thermodynamic activities of chromium and vanadium oxides were measured in the temperature range 1803−1923 K using an equilibration technique, where the slags containing low amounts of Cr or V ($CaO\text{-}MgO\text{-}Al_2O_3\text{-}SiO_2\text{-}CrO_x$ (or VO_x)) kept in Pt crucibles were equilibrated with a gas mixture of CO, CO_2 and Ar corresponding to well-defined oxygen partial pressures, which were kept very low. The experimental set-up is shown in Fig. 1

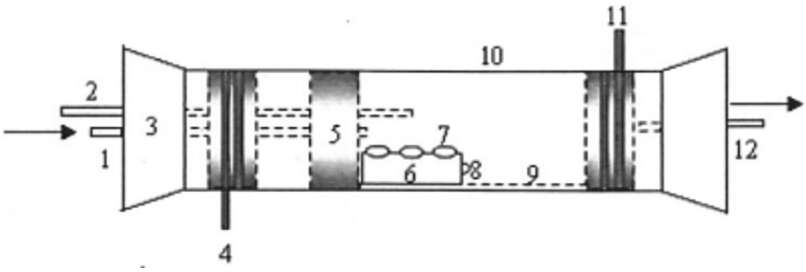

Fig. 1. The sketch diagram of the experimental equipment. 1. Gas inlet; 2. Thermocouple; 3. Silicon stopper; 4. Cooling water inlet; 5. Refractory; 6. Pure alumina holder; 7. Hole in the alumina holder for Pt crucibles; 8. Ceramic ring for pulling; 9. Alumina runners; 10. Reaction tube; 11. Cooling water outlet; 12. Gas outlet

The gases were purified suitably so that impurity oxygen levels were kept below 10^{-18} atm. The equilibration was carried out for a maximum of 20 h. The transition metal oxides were to be at their lowest oxidation states (Cr as Cr^{2+} and V as V^{3+}) due to the low oxygen potentials involved.

From the results, the activities of CrO and $VO_{1.5}$ were calculated with a knowledge of the thermodynamics of Pt-Cr and Pt-V alloys respectively. The activities showed positive deviation from Raoult's law in the case of CrO and negative deviation in the case of $VO_{1.5}$ as shown in Fig. 2. The standard states are pure CrO and $VO_{1.5}$ in liquid state.

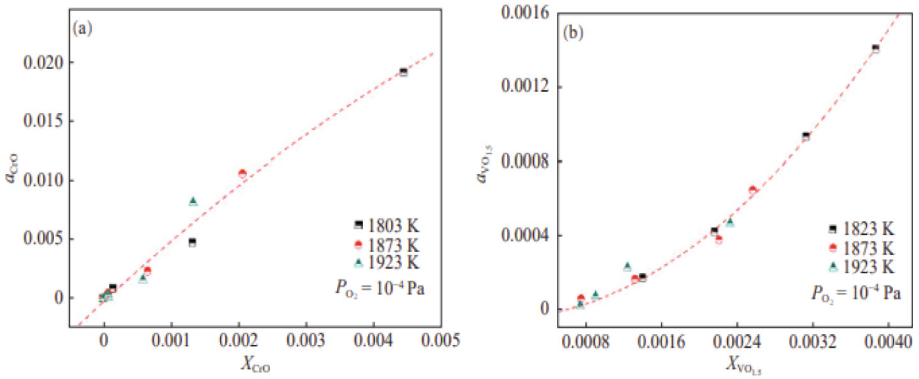

(a) (b)

Fig. 2. Thermodynamic activities of CrO (2a)[2] and VO1.5 (2b)[3] at various temperatures. The standard states are pure liquids at the experimental temperatures.

Valence States of the Oxides of Cr and V in Slags

An understanding of the chemistry of alloy steel slags under the operation conditions with varying temperatures and oxygen partial pressures, it is very important to have a knowledge of the valence states of the transition metals in the slag, specifically the oxides of Cr and V. The data available in literature were contradictory. The main problem is to analyze the slags after the experimentation without any oxidation during the chemical analysis, which otherwise would distort the results. Two new novel techniques were employed, one involving the X-ray Analysis Near Edge Spectroscopy (XANES) method, used mostly by geologists. The slags with suitable compositions were premelted and the compositions were determined accurately. The samples were subjected to XANES investigations [4, 5]. The other method was a new approach using the results of High Temperature Knudsen Cell Mass Spectrometric method [4, 6]. The mass spectrometry method which is a common method for measuring the vapour species was used for the first time to determine the valence states of transition metals in slag. The principles involved have been explained in the original publication 4. The results of the XANES studies are presented in Fig. 3.

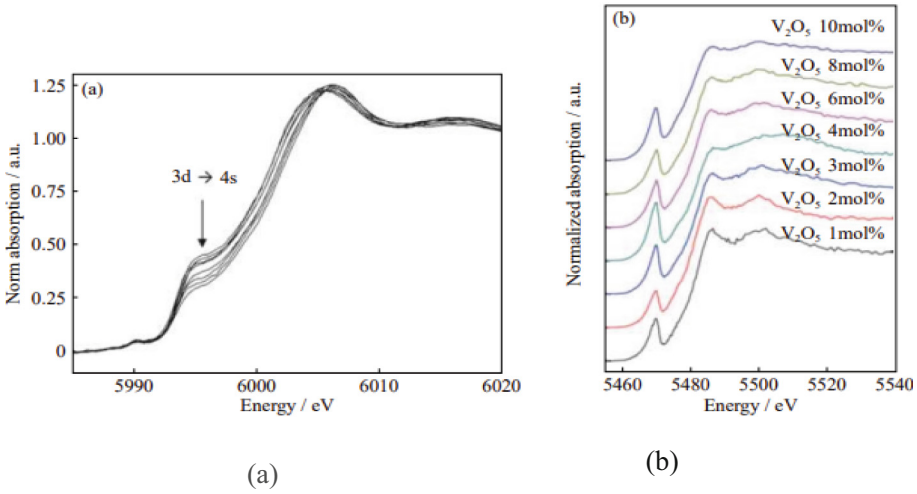

Fig. 3. XANES investigation results in the case of Cr (3a) and V (3b) slags [4, 5].

The ratio of Cr^{2+}/Cr^{3+} as functions of basicity as obtained by both the techniques is summarized in Fig. 4.

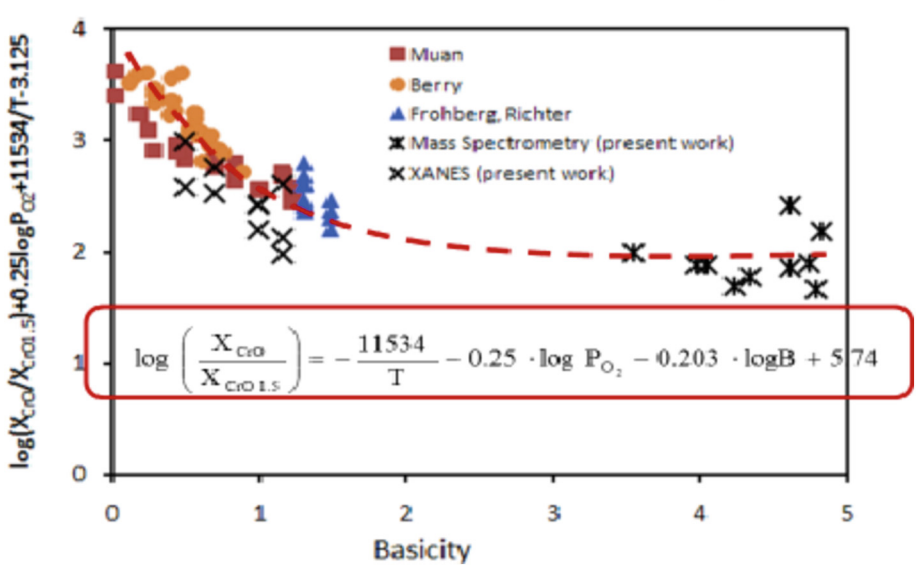

Fig. 4. The Cr^{2+}/Cr^{3+} ratio as a function of the basicity in Cr-containing steel slags 4.Similar results were ported in the case of vanadium-containing slags.

With a knowledge of the valence states of Cr in the slags as functions of temperature, oxygen partial pressure and basicity, it was now possible to understand the sulphide capacities of of these slags. As Cr_2O_3 is a surface-active oxide in slags, there would be an accumulation of this oxide in slag surfaces. It was found by XPS analysis that conventional sulphide capacity measurement provide only an average value of the sulphide capacities, whereas the oxidation state of sulphur varied from + 8 close to the gas/slag interface to −2 in the bulk of the slag.

Cr and V Emissions From Slags

It is known that both CrO_3 and V_2O_5 have high vapour pressures at steelmaking temperatures. Since CrO_3 is extremely carcerogenic, it is important to understand the emissions of CrO_3 when steel slags are tapped. The Single Hot Thermocouple Technique (SHTT) available at Bergakademie, Freiberg Germany was employed to study the evaporation from thin slag films. These slag films in the loop of the thermocouple (which is used both as a heater as well as for temperature measurement) were heated in air or oxygen to steelmaking temperatures and the loss of Cr or V was estimated after quenching using SEM/EDS method. The loss of Cr from chromium slags and V from vanadium slags are presented in Fig. 5(a) and (b) respectively.

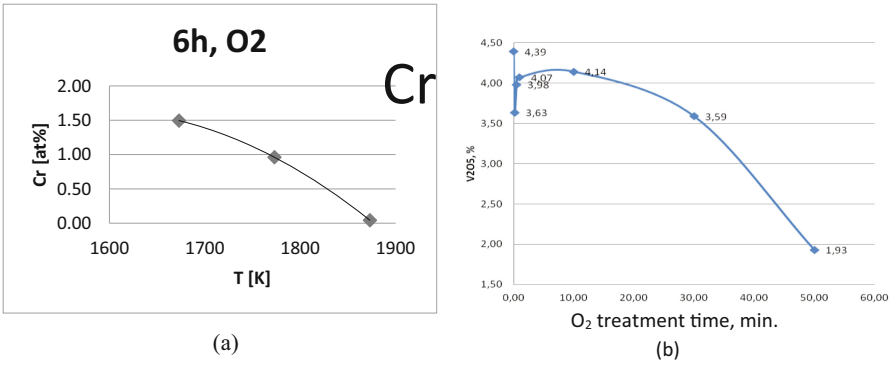

Fig. 5. Cr (5a)[7] and V (5b)[8] losses from slags after heating in air at steelmaking temperatures. T = 1873 K for vanadium experiments

This method has further been developed in the case of vanadium to recover this valuable metal from converter slags and other secondary resources 9.

Summary

The thermodynamic activities of Cr and V in steel slags were measured by a gas equilibration method involving CO-CO_2-Ar mixtures at molten steel temperatures.

The valence states of Cr and V in steel slags were measured by XANES method as well as high temperature Knudsen cell mass spectrometry.

The emission of CrO_3 and V_2O_5 from thin films of molten steel slags were studied by SHTT method. The method is now developed for commercial extraction of vanadium from lean sources and steel slags.

Acknowledgements. My sincere thanks to the organizers of METCENT for the opportunity to present our results. The contributions by various co-workers in obtaining the results reported are gratefully acknowledged.

References

1. Final Report, Eco Steel Production, Swedish Steel Producers Association (2012)
2. Dong, P., Wang, X., Seetharaman, S.: Thermodynamic activity of chromium, vanadium oxide in CaO-SiO2-MgO.Al2O3-CrOX slags. Steel Res. Int. **80**, 202−208 (2009)
3. Dong, P., Wang, X., Seetharaman, S.: Activity of VO1.5 in CaO-SiO2-MgO-Al2O3 slags at low vanadium contents and low oxygen pressures. Steel Res. Int. **80**, 251−255 (2009)
4. Wang, L.J., Seetharaman, S.: Experimental studies on the oxidation states of chromium oxides in slag phase. Metall. Mater. Trans. B **41**, 946–954 (2010)
5. Wang, H.J.: Investigations on thevoxidation of iron-chromium and iron-vanadium molten alloys, Ph. D. thesis, Royal Institute of Technology, Stockholm (2010)
6. Wang, L.J., Teng, L.D., Chou, K.C., Seetharaman, S.: Determination of vanadium valence state in CaO-MgO-Al2O3-SiO2 system by high temperature mass spectrometry. Metall. Mater. Trans. **44B**, 948–953 (2013)
7. Seetharaman, S., Albertsson, G., Scheller, P.R.: Studies of vaporization of chromium from thin slag films at steelmaking temperatures in oxidizing atmosphere. Metall. Mater. Trans. B **44**, 1280–1286 (2013)
8. Seetharaman, S., Shyrokykh, T., Schroeder, C., Scheller, P.R.: Vaporization studies from slag surfaces using a thin film technique. Metall. Mater. Trans. B **44**, 783–788 (2013)
9. Shyrokykh, T., Wei, X., Seetharaman, S., Volkova, O.: Vaporization of Vanadium Pentoxide from CaO-SiO2- VOx slags during alumina dissolution. Metall. Mater. Trans. B **52**, 1472–1483 (2021)

Solid State Reduction of Hematite Ore Using Hydrogen at Moderate Temperatures

Devendra Nama and Rahul Sarkar(✉)

Department of Materials Science and Engineering, Indian Institute of Technology Kanpur, UP 208016 Kalyanpur, Kanpur, India
{dnama20,rsarkar}@iitk.ac.in

Abstract. This work is carried out to investigate the reduction of hematite ore fines in a pure hydrogen atmosphere using thermogravimetric analysis (TGA). The effect of temperature (973-1173K) and hydrogen flow rate (1–2.5 L per minute) on the reduction kinetics was examined. The phases, morphological features, and chemical composition of hematite ore were identified using X-ray diffraction (XRD), Scanning electron microscopy (SEM), and X-ray fluorescence (XRF), respectively. The reduction kinetics were investigated using global reduction methods. The results show that the rate of reduction increases with temperature. An increase in hydrogen flow rate after the critical flow rate 2.5 LPM does not affect the rate of reduction. For global reduction, the reduction kinetics analysis indicates that the reduction was controlled by chemical mechanism. The apparent activation energy and preexponential factor for the global step are 20.4137 ± .22 kJ/mol and 0.7202 respectively.

Keywords: Hematite ore fines · hydrogen · TGA · reduction kinetics

1 Introduction

The BF-BOF routes is primarily responsible for producing steel. The coke is used as a reductant and source of energy in the blast furnace. It releases an enormous amount of carbon dioxide. The Iron and steel industry accounts for 7–9% of global carbon emissions [1]. Major economies are shifting towards net zero carbon emissions, so the Iron and steel industry is facing a lot of challenges to reduce its carbon footprint. To mitigate CO_2 emissions, several methods are suggested such as the partial substitution of fossil fuel with biomass [2], carbon capture and storage [3]. However, the drastic reduction in the emission is not possible from the existing technologies. The most promising way to reduce the carbon emissions from this sector is through the application of hydrogen-based direct reduction and hydrogen produced from electrolysis with renewable energy [4]. The new ironmaking technology needs to be developed that can reduce carbon emissions and take any type of iron ore in the form of fines as a raw input directly without the need for additional agglomeration procedures. It further decreases carbon emissions and energy consumption due to the exclusion of the agglomeration step [5].

S. Patra et al. (Eds.): METCENT 2023, *Proceedings of the International Conference on Metallurgical Engineering and Centenary Celebration*, pp. 19–27, 2024.
https://doi.org/10.1007/978-981-99-6863-3_3

A new ironmaking process will be developed which can convert the fines of iron ore concentrates into the iron in moving bed reactor by using reducing gas such as hydrogen or natural gas or coal gas at low temperatures. A schematic diagram of process is shown in the Fig. 1.

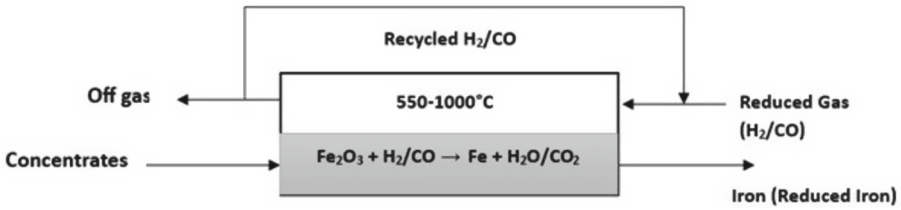

Fig. 1. Schematic diagram of possible ironmaking technology

When the hydrogen is used as a reductant then the conversion of hematite to iron occurs through the formation of intermediate oxides [6].

Fe_2O_3 (Hematite) → Fe_3O_4 (Magnetite) → Fe_xO (Wustite) → Fe (Iron) above 570 °C.

Fe_2O_3 (Hematite) → Fe_3O_4 (Magnetite) → Fe (Iron) below 570 °C [7].

These consecutive reactions, along with structural modifications in solids during reactions, increase the complexities. Many studies reported different activation energies and rate-controlling steps. The rate-controlling step varies with operational conditions and characteristics of solid particles such as shape, size, and mineralogical composition [8, 9].

In this study, the intrinsic kinetics of hematite ore reduction with hydrogen is experimentally determined. It is imperative to ensure that reduction must be carried out under such a condition in which the overall rate is controlled by the chemical kinetics. The influence of external mass transfer can be minimized by increasing the flow rate of gas past the sample. The influence of interparticle diffusion can be reduced by taking a thin layer of powder particles.

2 Experimental Methods

The isothermal reduction was carried out in the Thermo gravimetric analyzer (TGA). The schematic diagram of the setup is given in Fig. 1. It consisted of the vertical tubular furnace equipped with a micro weighing balance (accuracy 0.1mg) which is connected with a suspended crucible via a Kanthal wire. The Hematite concentrates were placed on the alumina crucible and the initial weight is recorded. The furnace was heated to set the temperature in the Nitrogen atmosphere. When the desired temperature is reached, hydrogen gas replaces the inert gas, and a computer-connected balance is used to continuously record the sample's weight. When there was no discernible change in the weight then reducing gas was replaced by nitrogen gas. Once the furnace had cooled to ambient temperature under the nitrogen atmosphere, the sample was removed and characterised (Fig. 2).